

Figure 29: Smaller TLV for defect 1054

## Self-supervised ML of boundary conditions in mechanics of materials

**D. Ryckelynck**

Th. Daniel, H. Launay, P. Pereira, H. Boukraichi, A. Aublet, S. Le Berre, D. Meshba, M. Bastico, A. Ferhat, P. Belamri

LJAD, November 20th 2025, LMA, December 2nd 2025, EHF2026

# SCIENTIFIC MACHINE LEARNING

The use of AI, especially generative AI, has become widespread in the daily lives of younger generations.

This comes with the following risks for science and technology:

**R1:** Loss of human expertise: AI can reproduce results or analyses based on pre-existing data, but it does not **understand** the scientific knowledge. AI is performing imitations. An erosion of engineers and researchers' skills who use AI could reduce their ability to innovate or solve complex problems. This risk can be countered by scientific machine learning that do not ignore this risk.

**R2:** Undetected biases and errors: AI models rely on databases that may contain biases, modeling errors, or gaps. Without human expertise to validate and interpret the results, critical errors could go unnoticed, with serious industrial or safety consequences. It is important to continue training experts with strong AI and applied mathematics skills in a **Human-Centered AI framework**.

**R3:** Excessive **standardization**: AI tends to favor solutions optimized for average cases. Care must be taken to build training databases where data variability has been favored.

**R4:** Technological dependence: Blind trust in AI tools could make industry players too dependent on these systems, reducing their autonomy.

**R5: Hindrance to knowledge transfer:** science is based on a scientific culture transmitted through teaching and practice. Engineers and researchers must continue to develop their **theoretical and practical skills**, integrating AI as a lever for analysis, not as a turnkey solution.



# SIMULATION IN MECHANICS OF MATERIALS AND MANUFACTURING PROCESSES

Simulation since the 60s :

- Reduce testing and empirical phases on real systems
- Provide predictions (with or without defects/damage)
- Modeling and understanding
  - Compare tests and predictions, address inverse problems
  - Perform sensitivity analysis
  - Get it right the first time
  - Optimize design and processes...

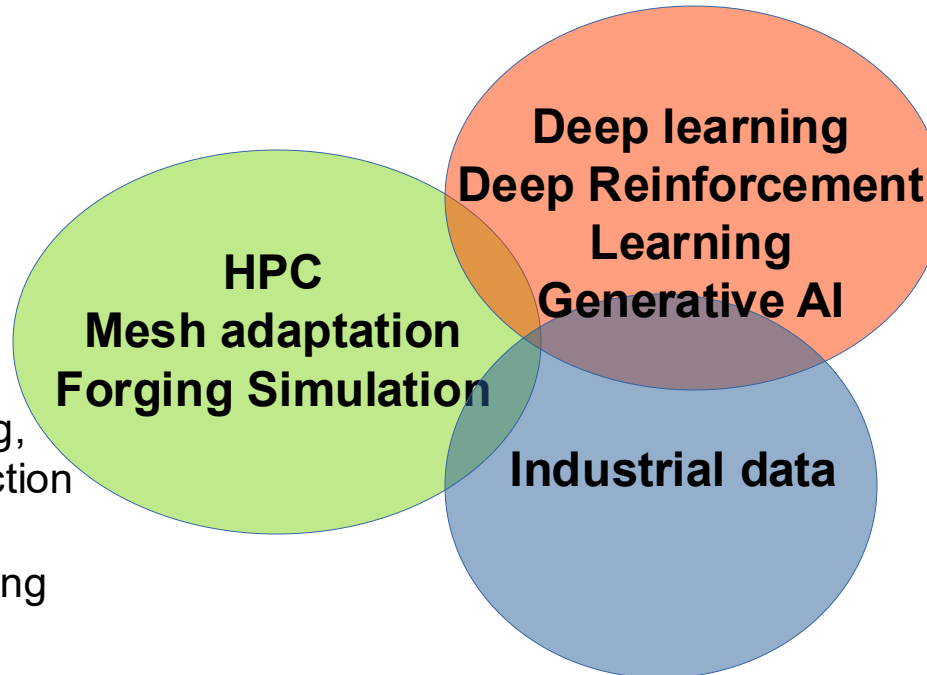
**Simulations are still too slow! HPC is not enough!**  
**Application of scientific knowledge is limited by its computational complexity!**  
**Predictions do not integrate new tasks enabled by AI.**

Since the 2000s model order reduction (in Zset, Aster, Cast3M, Ansys, without mesh adaptivity).

# INTEGRATING PHYSICS-BASED MODELING WITH AI

Fundamentally transforming the use of simulation through data and machine learning

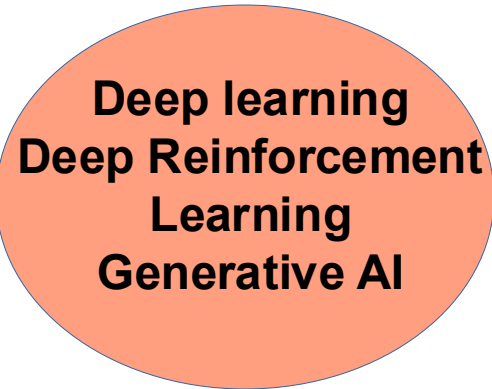
Hybrid AI  
Scientific Deep Learning



- Develop **new engineering tasks**
- Develop new **global and local indicators** such as anomaly index.
- ...
- Propose **contributions to XAI**

- **Assist** human for : digital twining, modeling constitutive laws or friction laws, train new collaborators ...
- **Automate and speedup** modeling task
- **Optimization**

# Machine Learning and Deep Learning



Main categories:

- Supervised machine learning,  **$Y(X)$  based on examples**  $(X, Y)$
- Unsupervised machine learning based on  $X$  (clustering, OOD...).
- Self-supervised machine learning,  **$Y(X) = X$** , pretrained models, dimensionality reduction...
- Reinforcement learning, optimization, autonomous systems...

Implementation steps:

- Choose an ambient space for data
- Save **datasets**
- **Augment data** in the train dataset
- Choose a neural network **architecture** and a **loss**
- **Train** the neural network
- **Test** the neural network

# Numerical example: void modeling in dilution condition and elasticity

Xindus = Image of a defect (48x48x1 tensor),  
 Y = 3 strain fields of 3 components related to 3 macroscopic loading

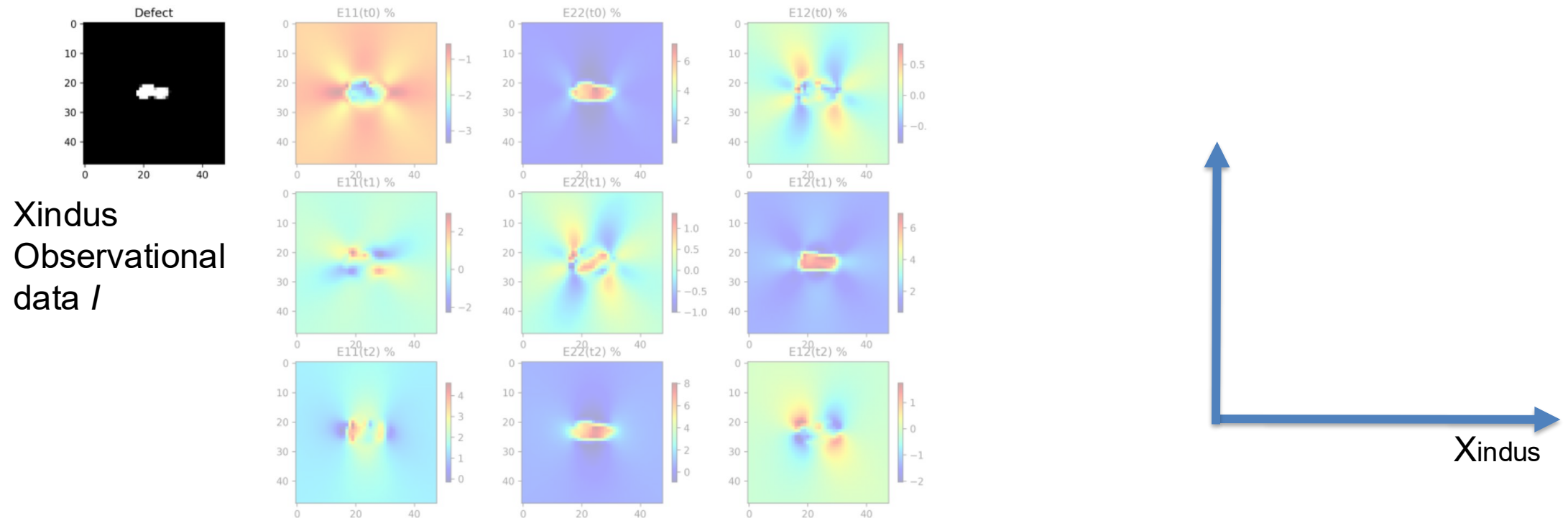
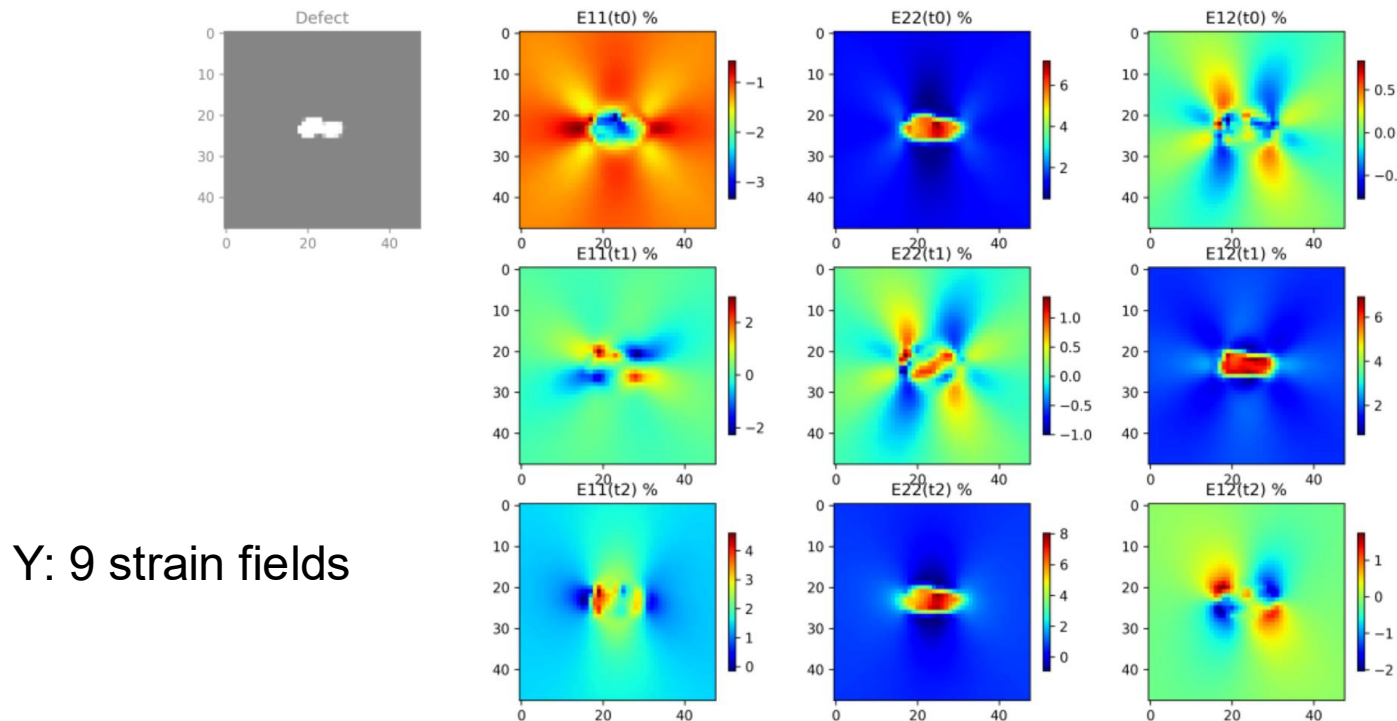


**Figure 6.** Strain components of the LROM for digital twin  $i = 1$ , on top left  $\mu_{\square}$ , on the right  $\varepsilon(\mathbf{V}^{(1)})$ . Here,  $t_0$ ,  $t_1$ ,  $t_2$  stand for the indices of the vectors that span the LROM.

# Numerical example: void modeling in dilution condition and elasticity

Xindus = Image of a defect (48x48x1 tensor),  
 Y = 3 strain fields of 3 components related to 3 macroscopic loading

Train a digital twin for strain predictions



Y: 9 strain fields

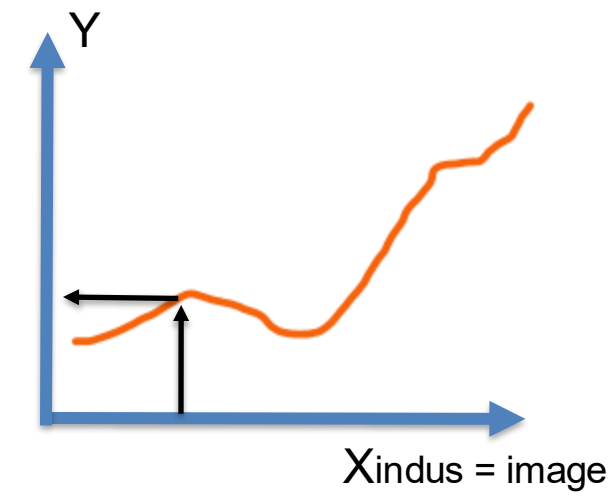
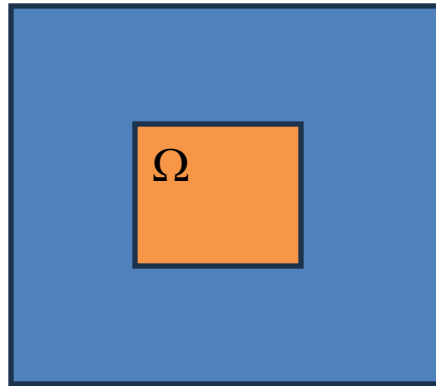


**Figure 6.** Strain components of the LROM for digital twin  $i = 1$ , on top left  $\mu_{\square}$ , on the right  $\varepsilon(\mathbf{V}^{(1)})$ . Here,  $t_0, t_1, t_2$  stand for the indices of the vectors that span the LROM.

# Theory: void modeling in dilation condition and elasticity



Domain for dilation  
condition  
Submodel

$$\operatorname{div}(\mathbf{C}(x) \varepsilon(\mathbf{u})) = f \quad \forall x \in \Omega, \quad \mathbf{u}(x) = \mathbf{u}_D(x) \quad \forall x \in \partial\Omega$$

Ellipticity

$$\alpha_{\Omega, \mathbf{C}} \|\mathbf{v}\|_{\Omega}^2 \leq \int_{\Omega} \operatorname{tr}(\varepsilon(\mathbf{v}) \mathbf{C} \varepsilon(\mathbf{v})) d\Omega \leq \gamma_{\Omega, \mathbf{C}} \|\mathbf{v}\|_{\Omega}^2$$

Coercivity  
 $\alpha_{\Omega, \mathbf{C}} > 0$

Continuity  
 $\gamma_{\Omega, \mathbf{C}} > 0$

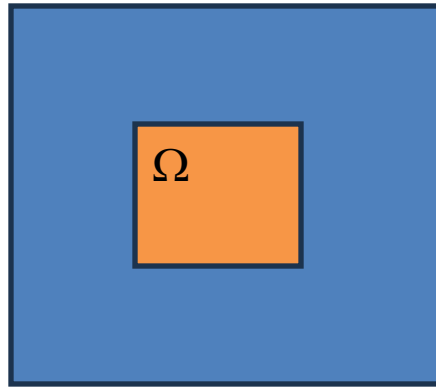
Target application for computer vision:

$$I \rightarrow \Omega(I), \mathbf{C}(x; I), \mathbf{u}_D(x; I) \quad x \in \Omega(I)$$

Learning boundary condition  $\mathbf{u}_D(x; I)$ .

# Theory: void modeling in dilution condition and elasticity

$$\operatorname{div}(\mathbf{C}(x) \varepsilon(\mathbf{u})) = f \quad \forall x \in \Omega, \quad \mathbf{u}(x) = \mathbf{u}_D(x) \quad \forall x \in \partial\Omega$$



Domain for dilution condition  
Submodel

FE modeling :  $\mathbf{K}\mathbf{q} = \mathbf{F}$

$$\mathbf{u}(x; I) = \sum_i \boldsymbol{\varphi}_i(x; I) q_i(I) + E x + \mathbf{r}(\mathbf{u}_D(I))$$

$$K_{ij}(x; I) = \int_{\Omega(I)} \operatorname{tr} \left( \varepsilon(\boldsymbol{\varphi}_i) \mathbf{C}(x; I) \varepsilon(\boldsymbol{\varphi}_j) \right) d\Omega$$

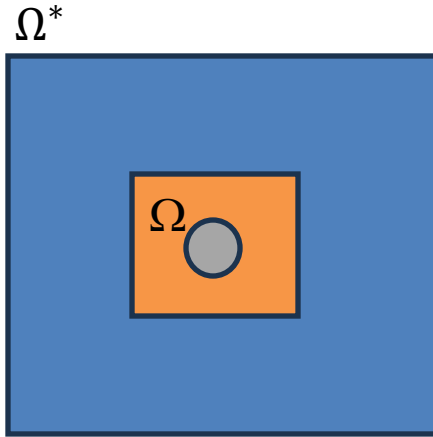
$$\tilde{\alpha} \|\mathbf{q}\|_2^2 \leq \mathbf{q}^T \mathbf{K} \mathbf{q} \leq \tilde{\gamma} \|\mathbf{q}\|_2^2$$

$$F_i(I) = - \int_{\Omega(I)} \operatorname{tr} \left( \varepsilon(\boldsymbol{\varphi}_i) \mathbf{C}(x; I) \left( E + \varepsilon \left( \mathbf{r}(\mathbf{u}_D(I)) \right) \right) \right) d\Omega = (\mathbf{F}_o + \mathbf{B}\mathbf{u}_D)_i$$

FE fluctuation  
+ macro strain  
+ filtering of boundary condition  
+ periodic coefficients

# Theory: void modeling in dilation condition and elasticity

$$\mathbf{u}(x; I) = \sum_i \varphi_i(x; I) q_i(I) + E x + \mathbf{r}(\mathbf{u}_D(I))$$



● Zone of interest

## Application of **Saint-Venant's principle**

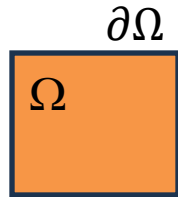
Under dilation conditions, for  $\Omega^*$  sufficiently large and far from an area of interest, the solution  $\mathbf{u}(x; I)$  is independent of the lifting  $\mathbf{r}(\mathbf{u}_D(I))$ . (See asymptotic properties of Green's functions [Blanc et al. 2013]\*.)

Definition :  $\mathbf{u}_D(I)$  is related to the solution under dilation condition restrained to a given sub-domain  $\Omega$ .

\*[[X. Blanc et al. 2013](#)]

# Theory: void modeling in dilution condition and elasticity

$$\mathbf{u}(x; I) = \sum_i \boldsymbol{\varphi}_i(x; I) q_i(I) + E x + \mathbf{r}(\mathbf{u}_D(I))$$



Deep learning predictions:

$$\begin{aligned} &\mathbf{u}_{ANN}(I) \text{ on } \partial\Omega, \\ &\mathbf{r}_{ANN}(I) \text{ over } \Omega \end{aligned}$$

Errors  $e_D(I) = \|\mathbf{u}_D - \mathbf{u}_{ANN}\|_{\partial\Omega}$

$$e_r(I) = \|\mathbf{r}(\mathbf{u}_D) - \mathbf{r}_{ANN}\|_{\Omega}$$

$$e_u(I) = \|\mathbf{u} - \mathbf{u}(\mathbf{r}_{ANN})\|_{\Omega}$$

Right hand side term:

$$\delta \mathbf{F} = \mathbf{F}(I) - \mathbf{F}_{ANN}, F_{ANNi}(I) = - \int_{\Omega(I)} \text{tr} \left( \boldsymbol{\varepsilon}(\boldsymbol{\varphi}_i) \mathbf{C}(x; I) (E + \boldsymbol{\varepsilon}(\mathbf{r}_{ANN}(I))) \right) d\Omega$$

# Theory: void modeling in dilution condition and elasticity

$$\mathbf{u}(x; I) = \sum_i \boldsymbol{\varphi}_i(x; I) q_i(I) + E x + \mathbf{r}(\mathbf{u}_D(I))$$



## Convergence property

$$\frac{e_u}{\|\mathbf{u}\|_\Omega} \leq \sqrt{\frac{\tilde{\gamma}}{\tilde{\alpha}} \frac{\|\delta \mathbf{F}\|_2}{\|\mathbf{F}\|_2}} \leq \sqrt{\frac{\tilde{\gamma}}{\tilde{\alpha}} \frac{\|\mathbf{B}\|_2}{\|\mathbf{F}\|_2}} \|\mathbf{u}_D - \mathbf{u}_{ANN}\|_{\partial\Omega}$$

The better the prediction  $\mathbf{u}_{ANN}(I)$  on  $\partial\Omega$ , the better the submodel prediction.

The smaller the elements in the submodel, the larger  $\tilde{\gamma}$  and the upper bound.

# Data generation using a FE model

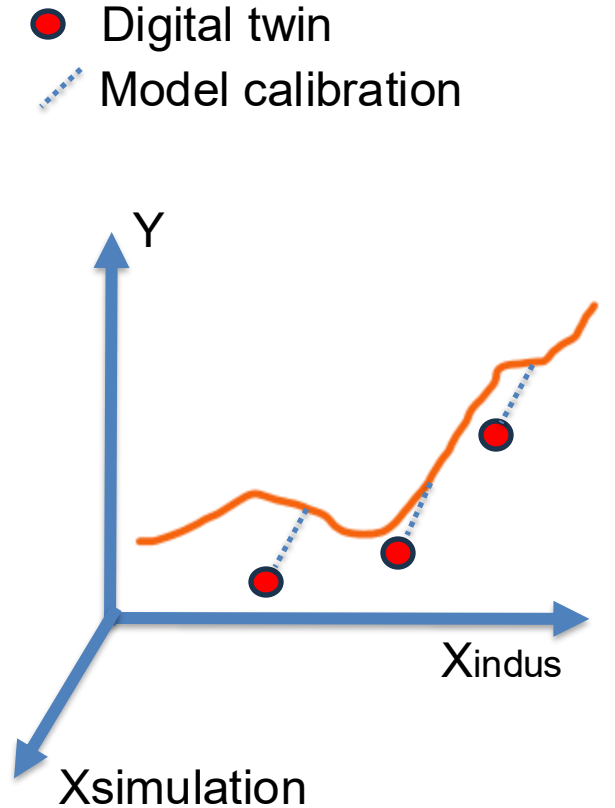
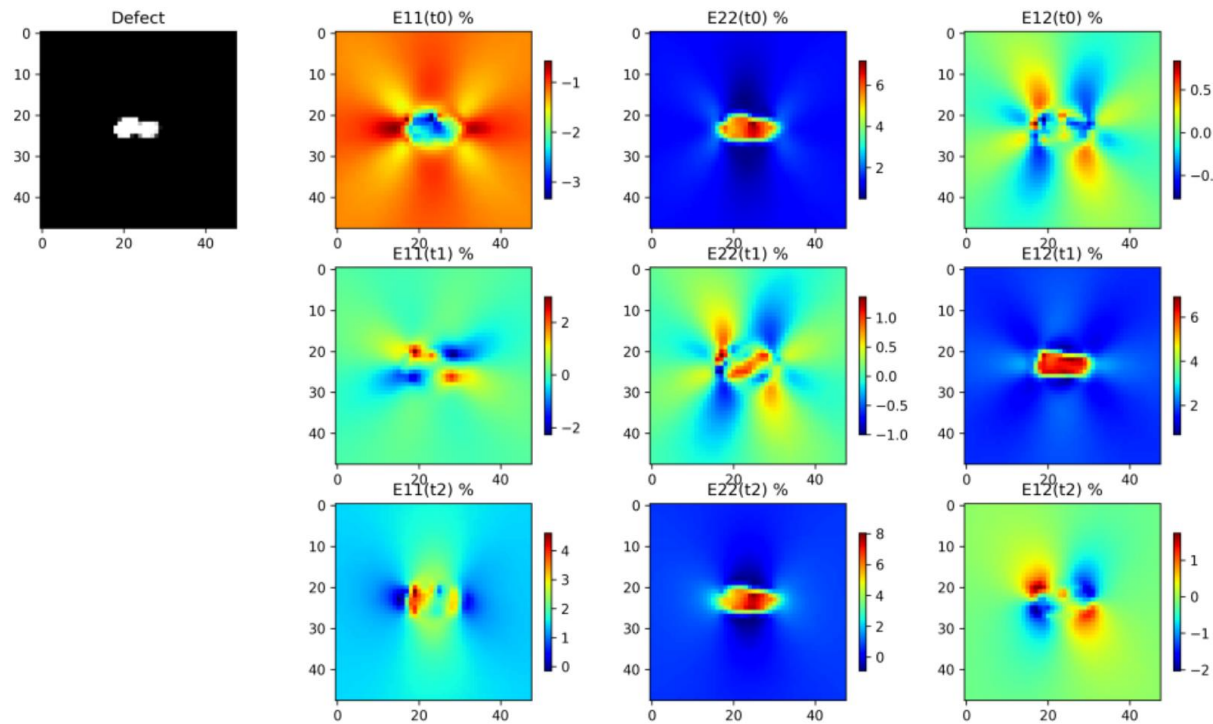


**Figure 6.** Strain components of the LROM for digital twin  $i = 1$ , on top left  $\mu_{\square}$ , on the right  $\varepsilon(\mathbf{V}^{(1)})$ . Here,  $t_0$ ,  $t_1$ ,  $t_2$  stand for the indices of the vectors that span the LROM.

# Data augmentation

Multimodal data augmentation for digital twinning assisted by artificial intelligence in mechanics of materials (2022)

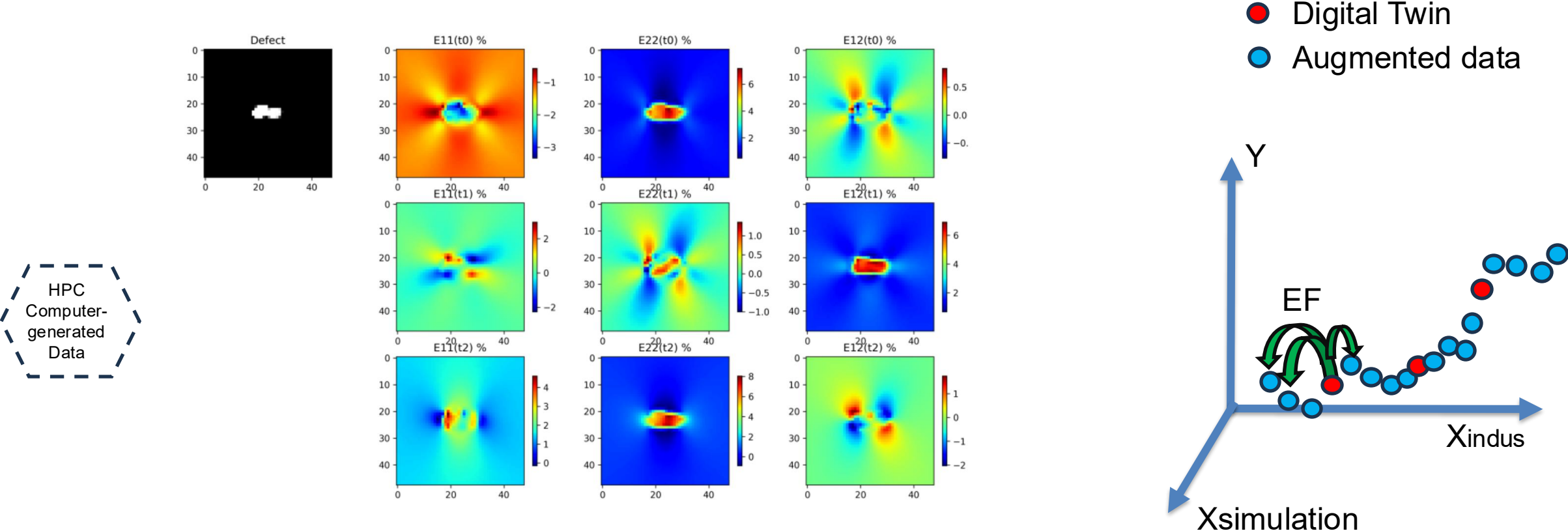
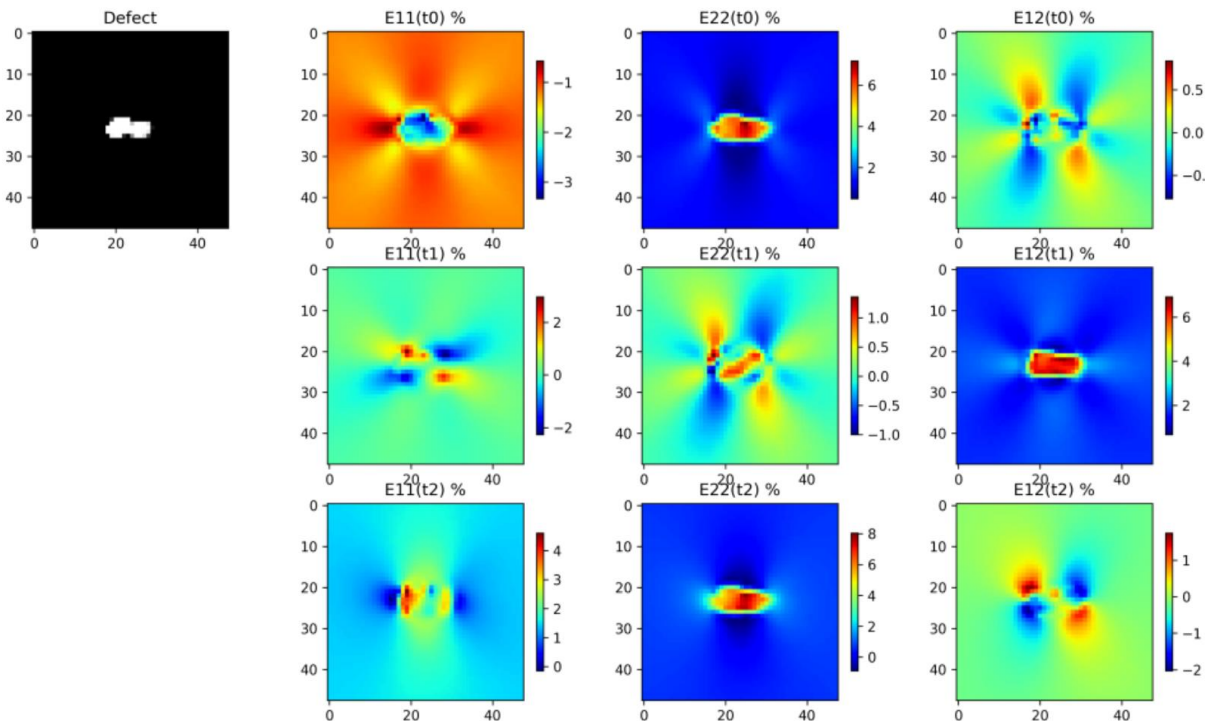


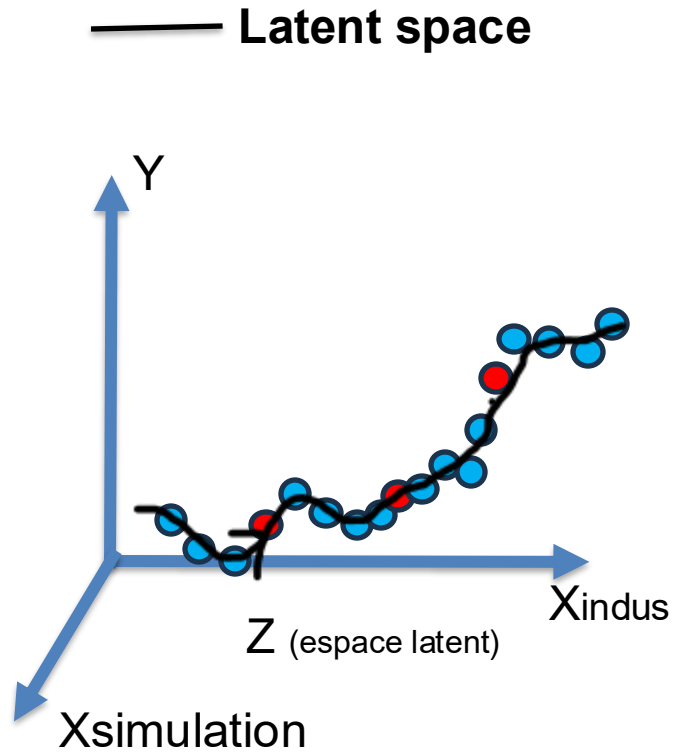
**Figure 6.** Strain components of the LROM for digital twin  $i = 1$ , on top left  $\mu_{\square}$ , on the right  $\varepsilon(\mathbf{V}^{(1)})$ . Here,  $t_0, t_1, t_2$  stand for the indices of the vectors that span the LROM.

# Self-supervised machine learning

Multimodal data augmentation for digital twinning assisted by artificial intelligence in mechanics of materials (2022)



Selfsupervised Learning

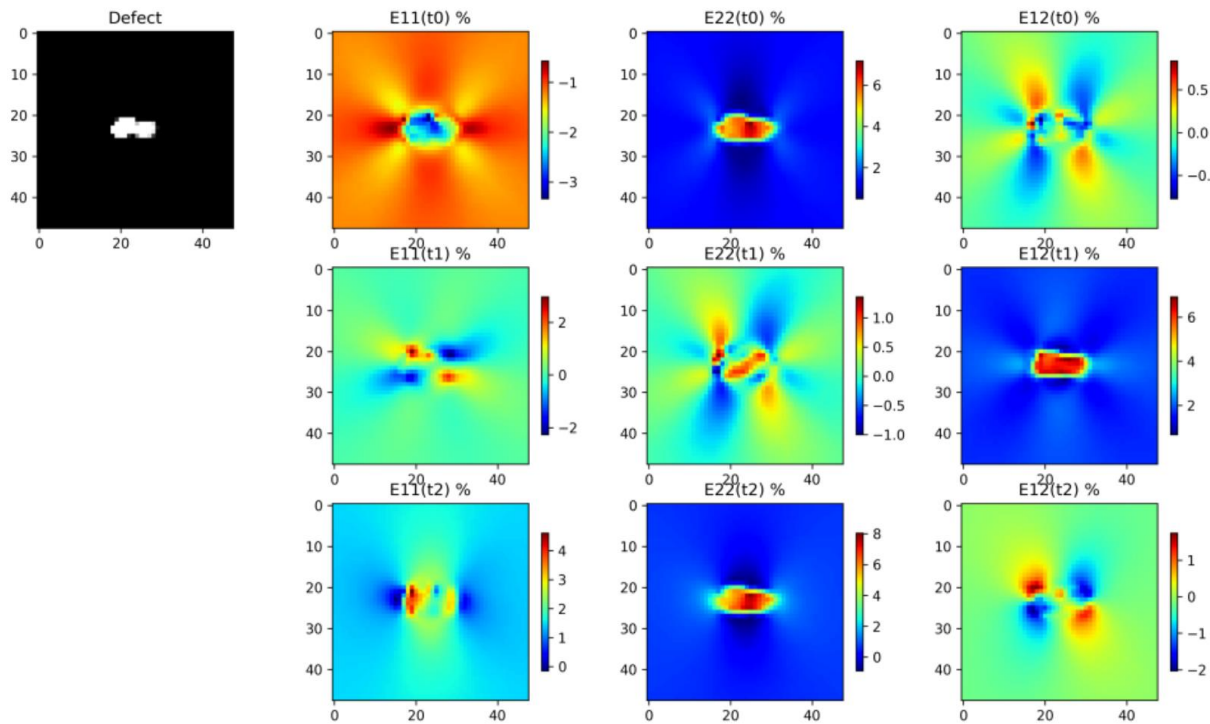


$$X_{multimodal} = ( X_{indus}, X_{simulation}, Y )$$

Z reduced coordinate

# Down stream task: Cross modal prediction

Metamodeling



Downstream task  
Regression  $Y(X)$ .

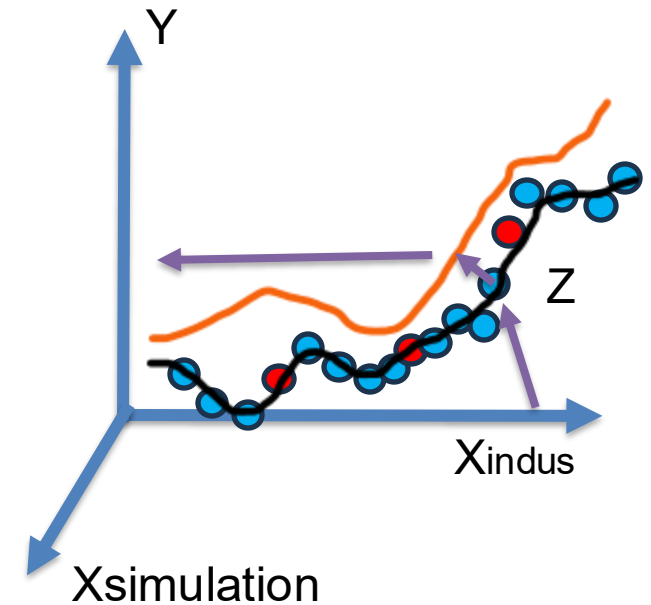
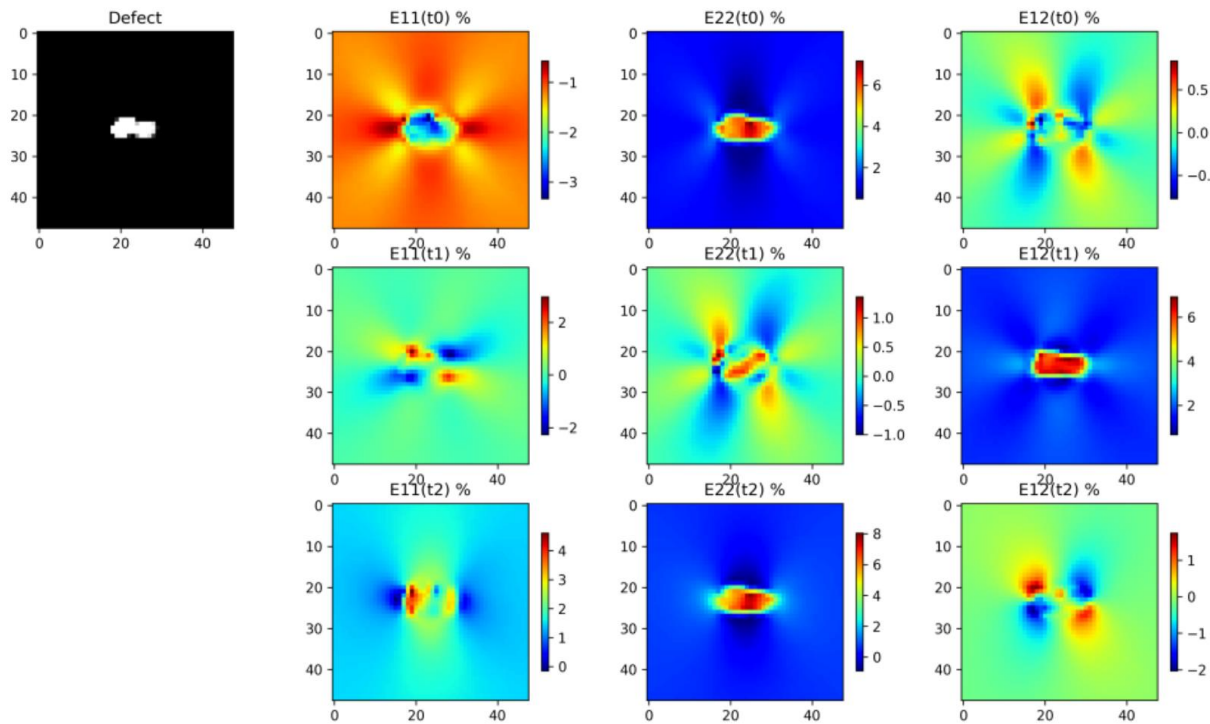


**Figure 6.** Strain components of the LROM for digital twin  $i = 1$ , on top left  $\mu_{\square}$ , on the right  $\varepsilon(\mathbf{V}^{(1)})$ . Here,  $t_0, t_1, t_2$  stand for the indices of the vectors that span the LROM.

# Down stream task: Cross modal prediction

Metamodeling



Downstream task  
Regression  $Y(X)$ .

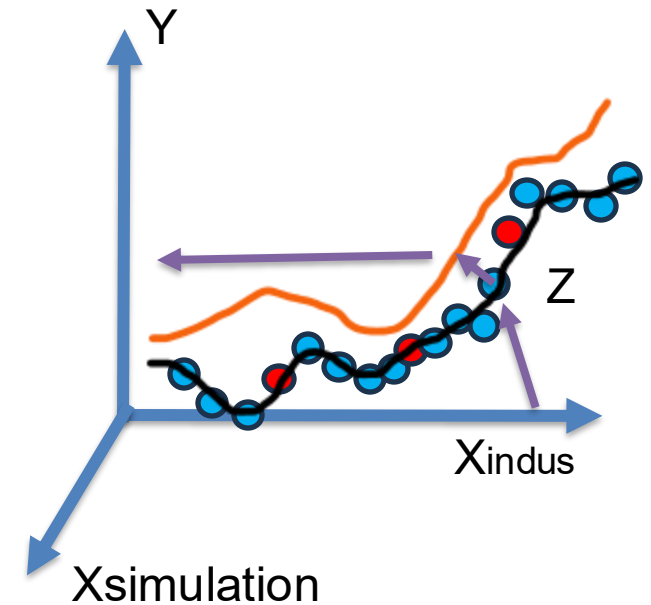
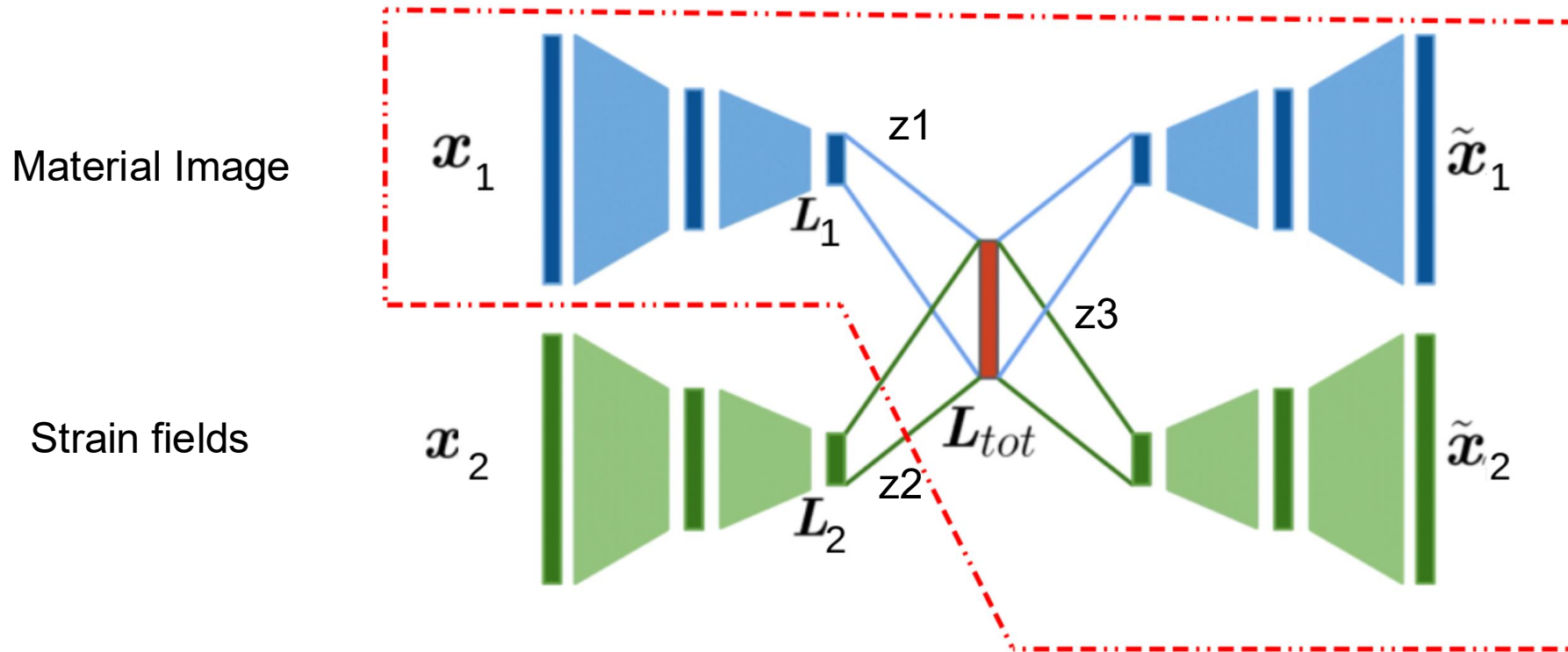


**Figure 6.** Strain components of the LROM for digital twin  $i = 1$ , on top left  $\mu_{\square}$ , on the right  $\varepsilon(\mathbf{V}^{(1)})$ . Here,  $t_0, t_1, t_2$  stand for the indices of the vectors that span the LROM.

# Model architecture for self-supervised machine learning on multimodal data

Dual encoder architecture



$$z_3 = (z_1 + z_2) / 2$$
$$L_{tot} = z_1 - z_2$$

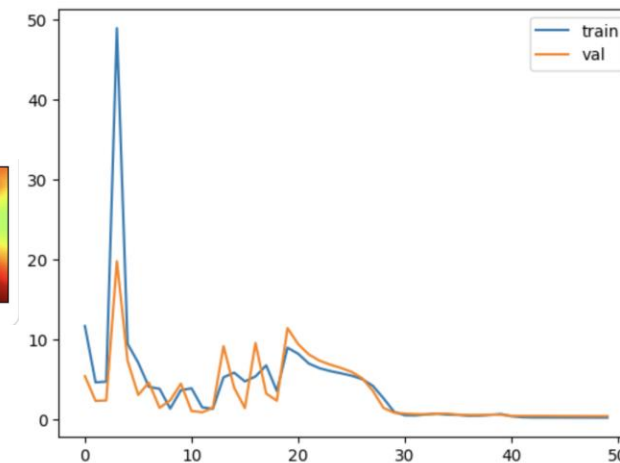
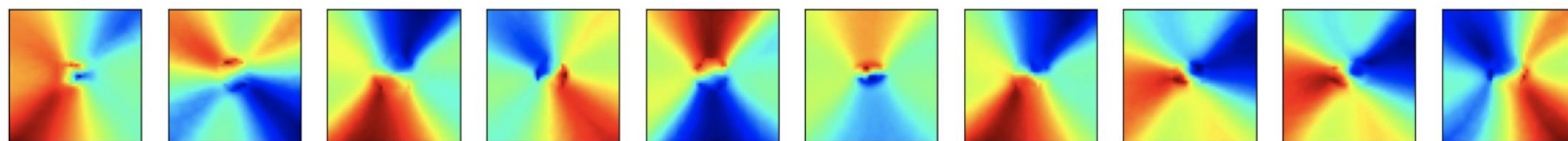
[Deep multimodal autoencoder for crack criticality assessment](#)

Hugo Launay , David Ryckelynck , Laurent Lacourt , Jacques Besson , Arnaud Mondon et al.

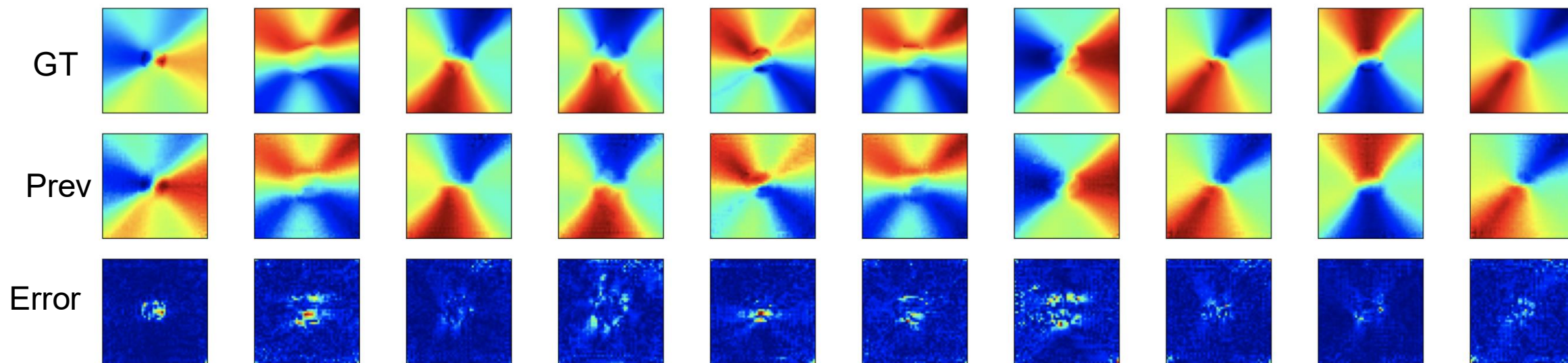
International Journal for Numerical Methods in Engineering, 2022, 123 (6), pp.1456-1480. [10.1002/nme.6905](https://doi.org/10.1002/nme.6905)

# Mechanical autoencoder for strain fields

Train dataset : 3000 strain fields



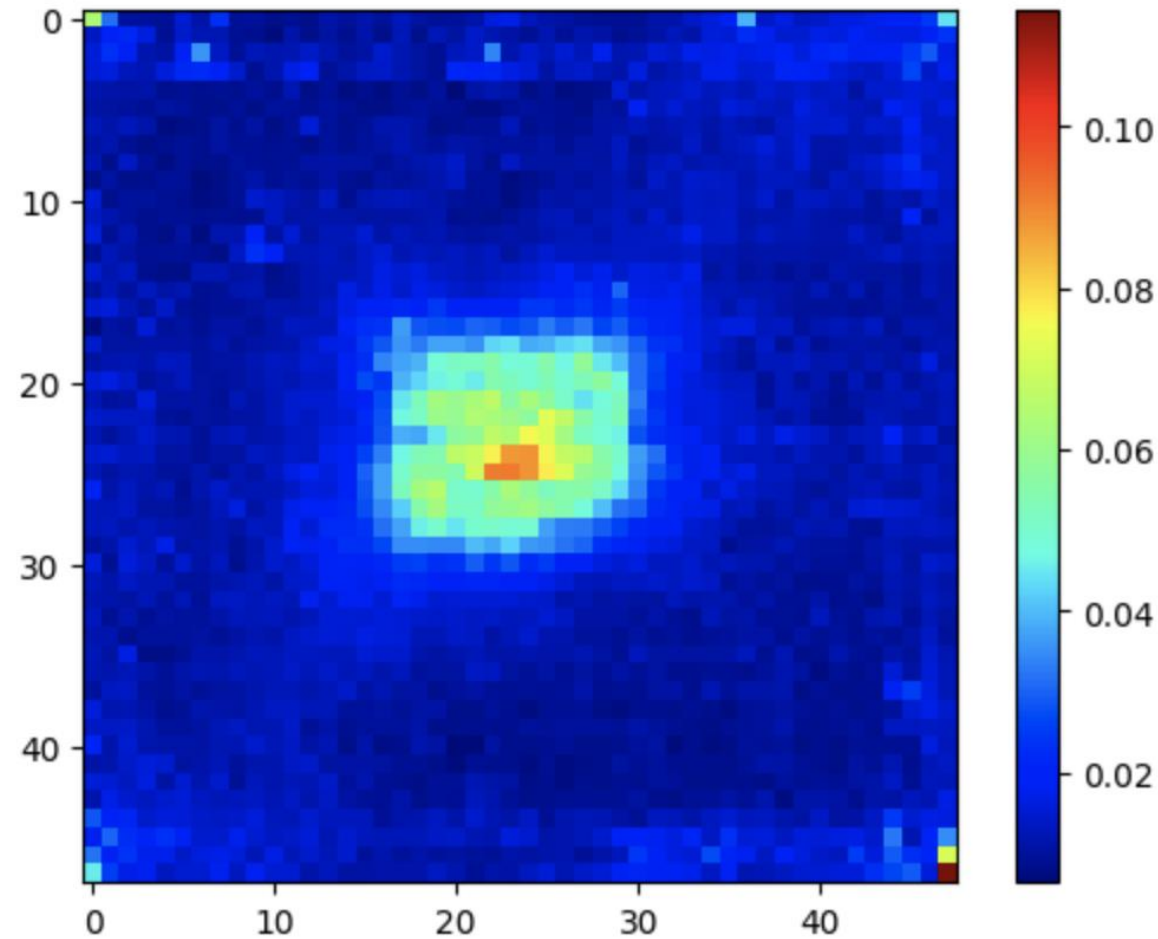
Test



# Mechanical autoencoder for strain fields



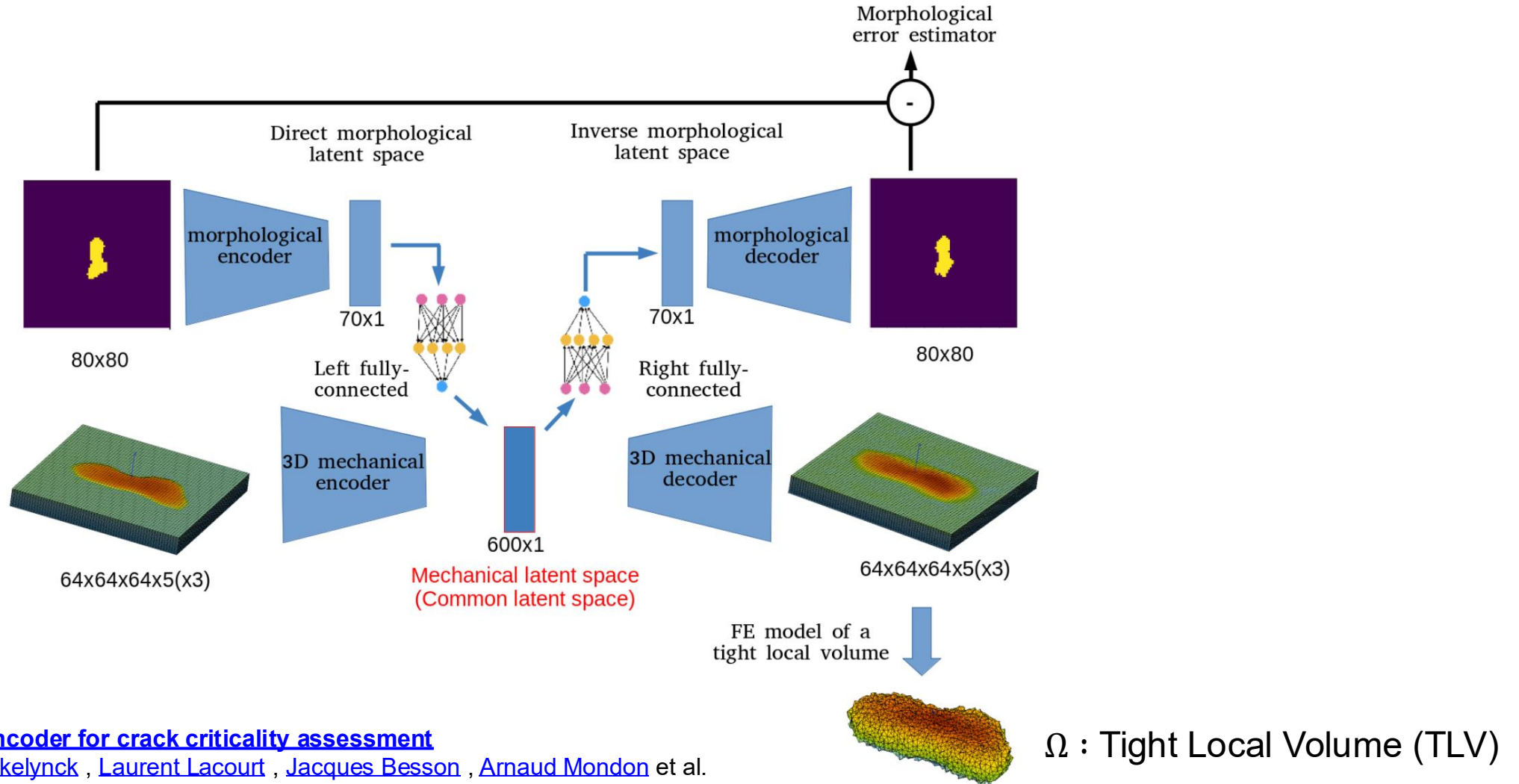
Map of local mean errors



Fully consistent with Saint-Venant's principle and FE submodeling.

# Multimodal autoencoder for FE submodeling

## Learning boundary condition for PDE



[Deep multimodal autoencoder for crack criticality assessment](#)

Hugo Launay, David Ryckelynck, Laurent Lacourt, Jacques Besson, Arnaud Mondon et al.

International Journal for Numerical Methods in Engineering, 2022, 123 (6), pp.1456-1480. [10.1002/nme.6905](https://doi.org/10.1002/nme.6905)

Figure 6: Modified MM Capture d'écran d error indicator to generate displacement field on TLV.

# Multimodal autoencoder for FE submodeling

## Digital Twin

2D crack in 3D volume

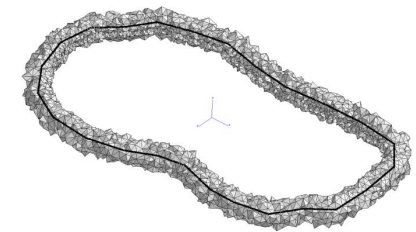
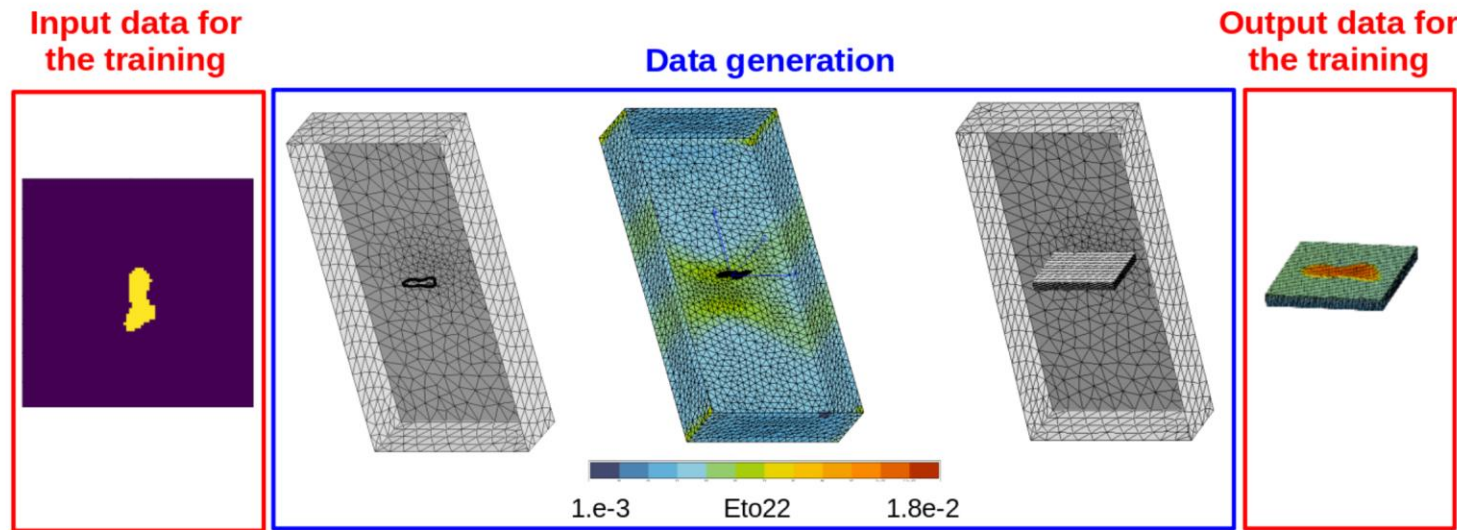


Figure 29: Smaller TLV for defect 1054

Tight Local Volume

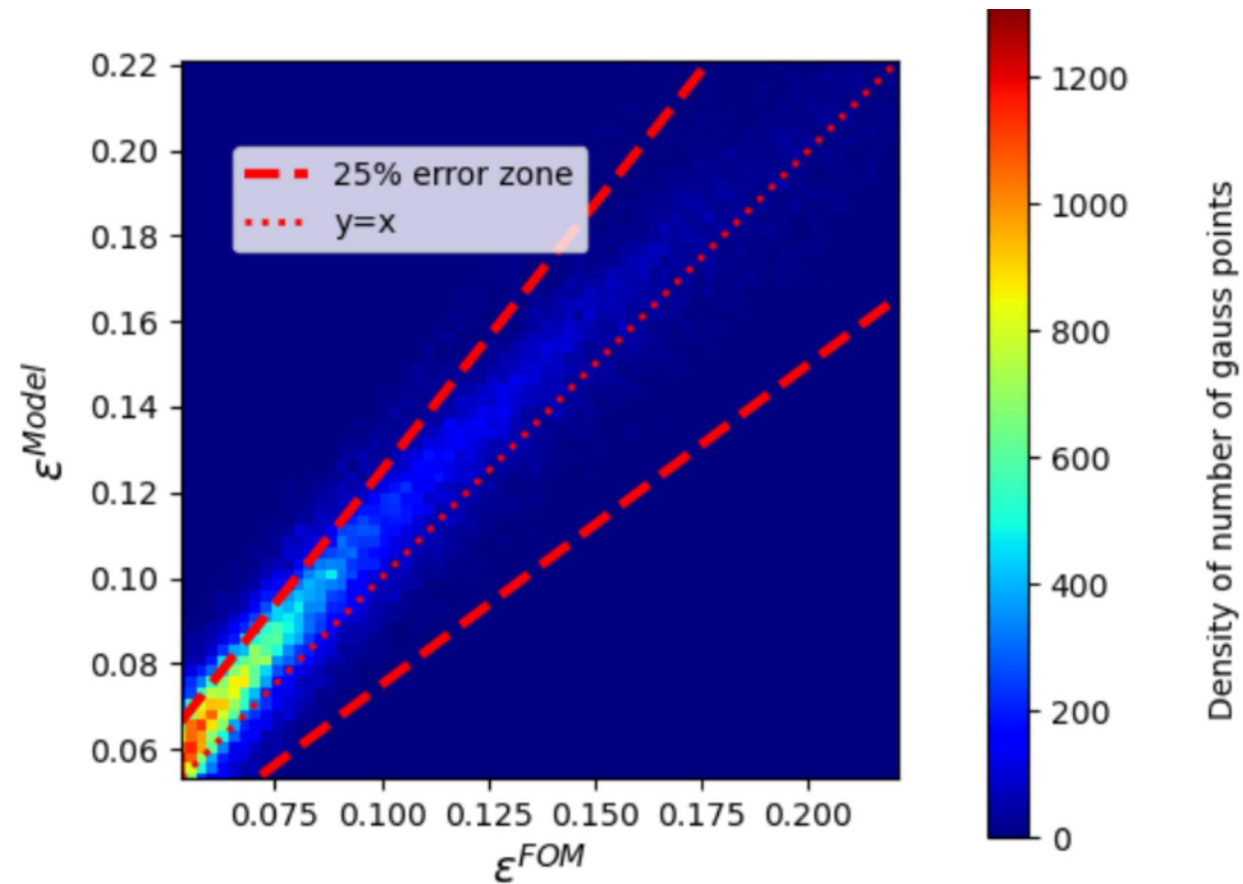
Figure 4: (a) 2D image representing the crack, (b) insertion of the 2D crack in the 3D mesh, (c)  $E_{22}$  field, (d) position of the encoding mesh in the full structure and (e) the encoding mesh with the transferred information.

Train dataset



# Multimodal autoencoder for FE submodeling

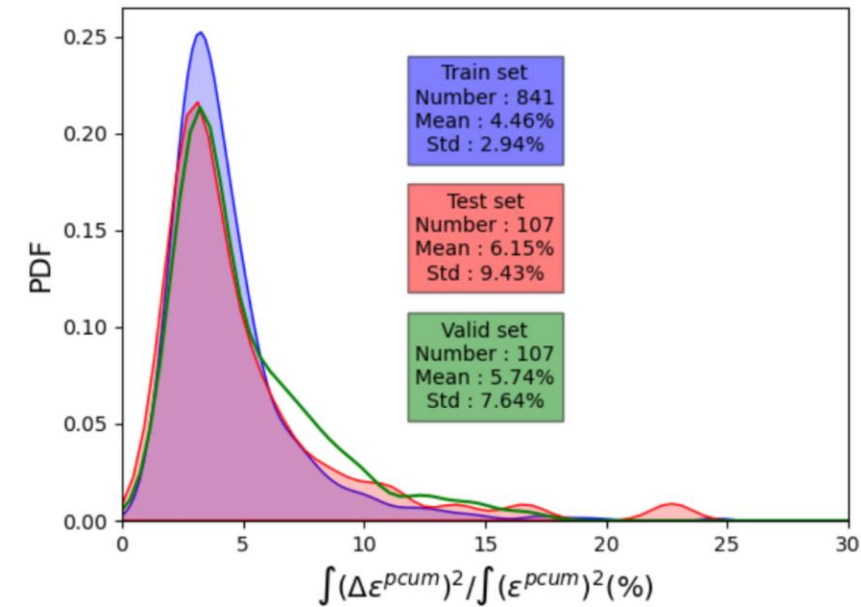
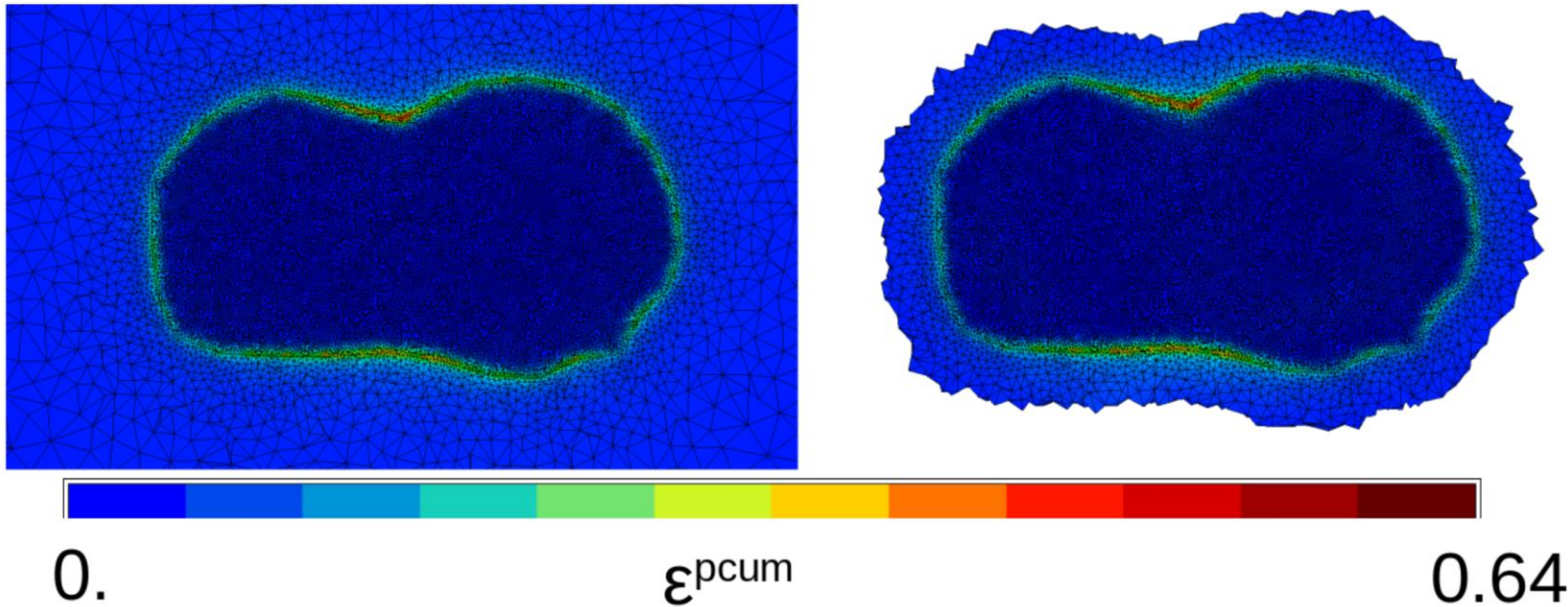
## A posteriori error



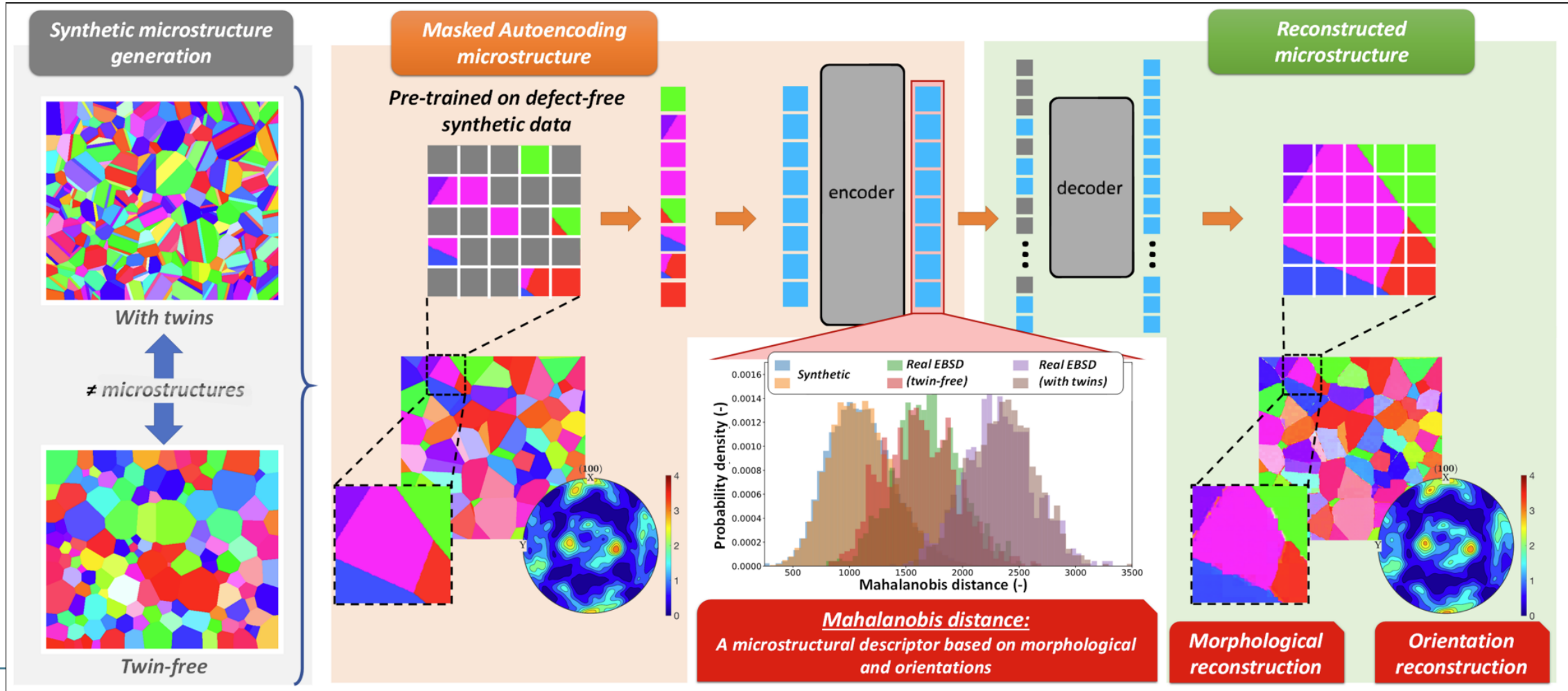
# Multimodal autoencoder for FE submodeling

## Generalisation error

Plasticity, isotropic hardening, speedup = 10



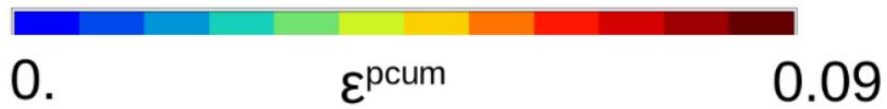
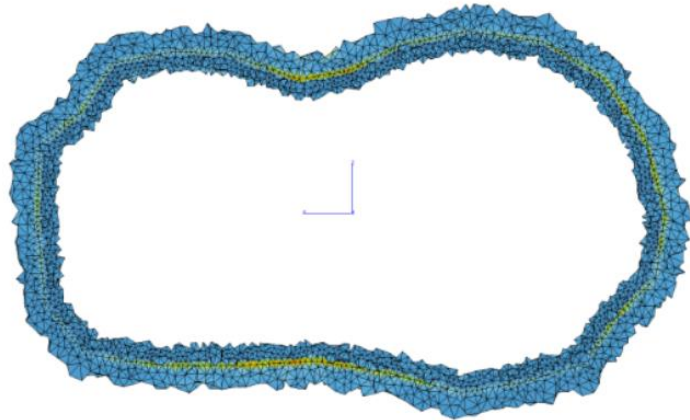
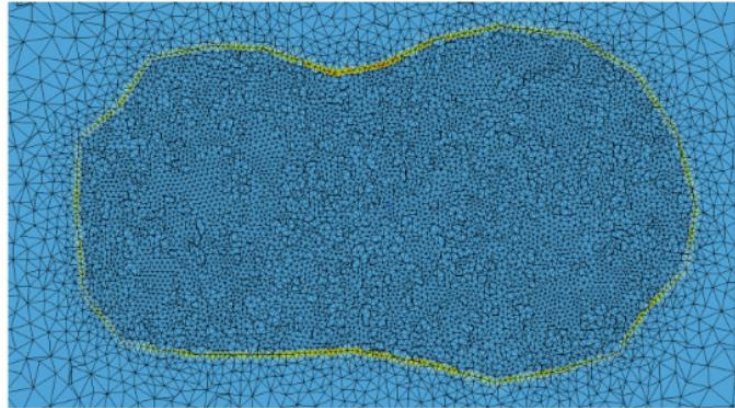
# Anomaly detection using autoencoder In crystal plasticity



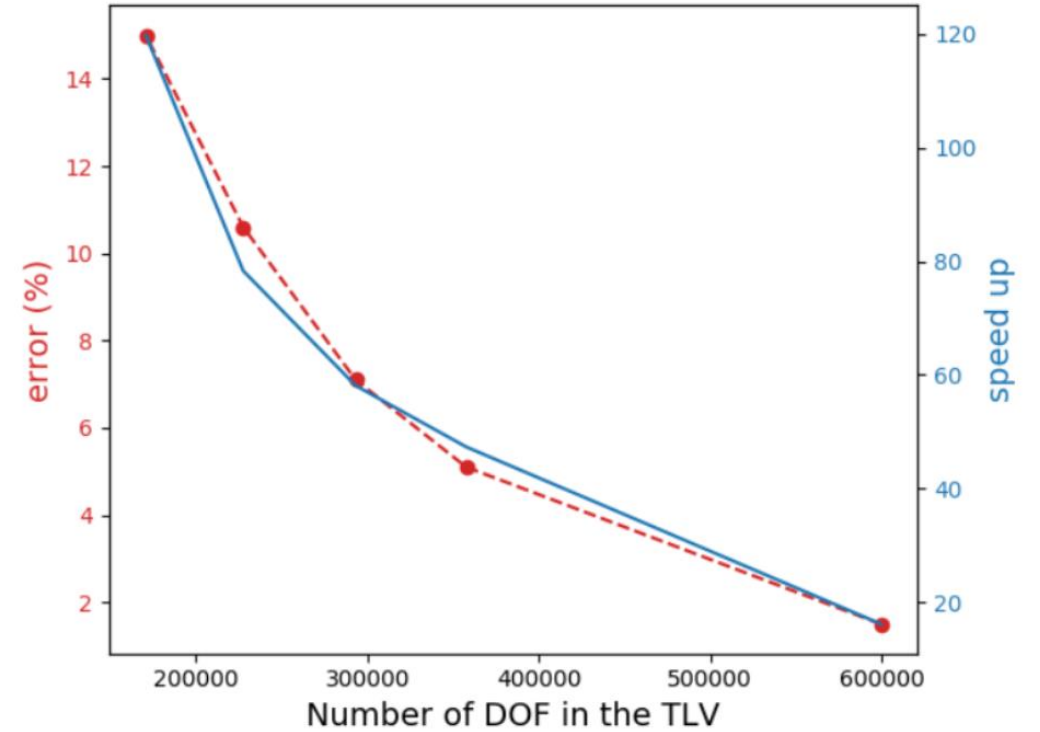
**Quaternion-Based Vision-Transformer for Polycrystalline EBSD Scans Pre-Trained on Large-Scale Synthetic Data**

Pierre Belamri , Henry Proudhon , Damien Texier , David Ryckelynck  
Materials & Design, 2025, 258, pp.114599. ([10.1016/j.matdes.2025.114599](https://doi.org/10.1016/j.matdes.2025.114599))

# Conclusion



Toward XAI using FE submodels



(b)

# Numerical practice



Requirement : Internet access and Google Drive

Create a working directory on your Google Drive.

Download `Load_PyTorch_Convolutional_Autoencoder_Solution.ipynb` in this directory.

Open this file with Google Collaboratory

Run `Load_PyTorch_Convolutional_Autoencoder_Solution.ipynb`

Download `PyTorch_Convolutional_Autoencoder_Solution.ipynb`

Open

Work to do :

Compute the reconstruction error on the boundary of a square of dimension  $a=[5,\dots,25]$ .

Plot the average error on this boundary as a function of  $a$ .

Comment with respect to de Saint Venant's Principle